Journal of Sound and Vibration (2001) **242**(3), 487–505
doi:10.1006/jsvi.2000.3356, available online at http://www.idealibrary.com on IDEAL®

THE INFLUENCE OF ROTATION ON VIBRATION OF A THICK CYLINDRICAL SHELL

D. GUO AND F. L. CHU

State Key Laboratory of Tribology, Department of Precision Instruments, Tsinghua University, Beijing 100084, People's Republic of China

AND

Z. C. ZHENG

Department of Engineering Mechanics, Tsinghua University, Beijing 100084, *People's Republic of China*

(*Received* 8 *December* 1999, *and in final form* 1 *October* 2000)

The problems of the vibration of rotating cylindrical shells are solved by using nine-node super-parametric finite element with shear and axial deformation and rotatory inertial. The non-linear plate-shell theory for large deflection is used to handle the cylindrical shell before it reaches equilibrium state by centrifugal force. The effects of Coriolis acceleration, centrifugal force, initial tension and geometric non-linearity due to large deformation are considered in this model. Eight categories of mode of a rotating thick cylindrical shell are presented. The effects of rotation on different three-dimensional modes of cylindrical shell are discussed in detail.

1. INTRODUCTION

T'here are many engineering applications resulting from studies involving the vibration of shells. This has been extended to studies on the vibration of rotating cylindrical shell as there are also engineering application of a rotating shell in industry, for example, in the drive shafts of gas turbines, motors and rotor system.

The earliest recorded work on rotating cylindrical shells was by Bryan [1], in which the free vibration of a rotating cylindrical shell was considered and the phenomenon of travelling modes was also discovered. Early works on rotating shells included the study of the Coriolis effect on the free vibration by Taranto and Lesson [2] and Srinivasan and Lauterbach [3] for infinite-length rotating shells and by Zohar and Aboudi [4] for finite-length rotating shells. Other works included the study of long rotating cylinders subjected to pre-stress by Padovan [5], the study of vibrations and buckling of rotating anisotropic shells by Padovan [6] and the study of multi-layered rotating cylinders by Padovan [7]. Saito and Endo [8] considered the effect of initial tensions. Endo *et al*., [9] studied the flexural vibration of a thin rotating cylindrical ring especially from the experimental point of view, and compared the results of experiment with that of theory. Recently, the free vibrations of rotating composite shells have been studied by Rand and Stavsky [10]. Extensive works on the vibration of cylindrical shell, both stationary and rotating, have been carried out by Lam, etc. Analysis of rotating laminated cylindrical shells using different thin shell theories have been carried out by Lam and Loy [11]. Studies have also been carried out on rotating laminated composite [12], sandwich-type cylindrical shells [13] and orthotropic shell [14], Furthermore, they have extended the study of rotating cylindrical shell to that of rotating conical shell [14–17]. A new numerical approximate method — GDQ method has been presented to study the effects of boundary conditions and initial pressure on the frequency characteristics [17, 18]. The resonance phenomena of rotating cylindrical shells subjected to a harmonic moving load or periodic axial loads have been studied by Huang and Hsu [19] and Ng and Lam [20].

It is difficult to solve the dynamic equation in general form by analytical method. For cylindrical shells and circular plates the series-form solutions can be found, but these are not convergent in general. For a cylindrical shell the analytical solutions are valid only for some particular boundary conditions. Numerical solutions can be found by finite element methods in the general case. These include the methods of Padovan [6], Chen *et al.* [21] and Sivadas [22, 23].

Most of the researchers used thin theory analyze rotating shells. Studies on rotating thick cylindrical shells are very limited. Sivadas and Ganesan [22] studied the vibration of rotating thick cylinders by an improved shell theory with shear deformation and rotatory inertia. But in their paper, no attempt was made to study the effect of rotation on three-dimensional modes of rotating cylinders.

In the past, most of the investigations have also provided information about mode shapes in order to obtain a complete understanding of the vibrations of thick cylinders. However, the mode shapes were generally described in the circumferential and longitudinal directions separately. The mode shape description is based on two parameters, n and m, where n is half the number of circumferential nodes, and m is the number of longitudinal nodes [24]. Such a method of mode description may be satisfactory for the vibrational modes of thin cylinders, but it is not complete enough to accurately describe the modes of thick cylinders. It can be seen from the same reference that several combinations of the same n and m existed in the frequency range investigated. It is clearly impossible for several frequencies to have exactly the same mode shape. Recently, Wang and Williams [25] proposed a different mode classification of finite-length thick cylinders, based on their three-dimensional mode shapes. Using this classification together with the descriptors n and m, all of the vibrational modes of finite-length thick cylinders can be identified uniquely. Hence, a better understanding of the vibrations of stationary thick cylinders can be obtained. However, extensive search of literature has thus far shown that no work on the three-dimensional mode shapes of a rotating thick cylinder has been carried out; hence, no studies on the effect of rotation on its different modes have been performed.

In order to overcome this drawback, this paper will study for the first time the effect of rotation on different three-dimensional modes of a thick cylndrical shell with F-F boundary condition using moderately thick shell theory. A nine-node superparametric finite element is used. This paper has deduced the finite element form of rotating cylindrical shells. The non-linear plate-shell theory for large deflection is used to handle the cylindrical shell before it reaches the equilibrium state by centrifugal force, and then a linear approximation is employed. Not only the effect of Coriolis acceleration, centrifugal force, and initial tension, but also the geometric non-linearity due to large deformation is considered in this model. To examine the accuracy of the present analysis, comparisons are made with the results in the open literature for non-rotating and rotating cylindrical shells.

2. THEORETICAL FORMULATION

The nine-node curvilinear finite element method is used in this paper. The following assumptions are made:

- "Normals" to the middle surface remain straight after deformation.
- The stress component normal to the shell mid-surface is constrained to be zero.

Each node point has five degrees of freedom: u, v and w are three displacement components; α and β are two rotational angles in $\bar{V}_1$ and $\bar{V}_2$ directions. The detailed forms of element description and derivation of the element stiffness matrix are available in the literature [26]. Only a brief presentation of finite element formulation for free vibration analysis is presented in the following.

The co-ordinates of a point within the element are obtained by applying the element shape functions to the nodal co-ordinates,

$$\begin{Bmatrix} x \\ y \\ z \end{Bmatrix} = \sum_{k=1}^{n} N_k \begin{Bmatrix} x_k \\ y_k \\ z_k \end{Bmatrix}_{midsurface} + \sum_{k=1}^{n} N_k \frac{h_k}{2} \varsigma \bar{V}_{3k}, \tag{1}$$

where n is the number of nodes per element: $N_k = N_k(\xi, \eta)$ $(k = 1, n)$ are the element shape functions corresponding to the surface $\varsigma =$ constant; h_k is the shell thickness at node k; ξ, η, ς are the curvilinear co-ordinates of the point.

The element displacements can be expressed by

$$\begin{Bmatrix} u \\ v \\ w \end{Bmatrix} = \sum_{k=1}^{n} N_k \begin{Bmatrix} u_k \\ v_k \\ w_k \end{Bmatrix}_{midsurface} + \sum_{k=1}^{n} N_k \varsigma \frac{h_k}{2} [\bar{V}_{1k} - \bar{V}_{2k}] \begin{bmatrix} \alpha_k \\ \beta_k \end{bmatrix}. \tag{2}$$

Equation (2) can be simply written as

$$\bar{\delta} = \begin{Bmatrix} u \\ v \\ w \end{Bmatrix} = N\bar{a}, \tag{3}$$

where

$$\bar{a} = \begin{Bmatrix} a_1 \\ a_2 \\ \vdots \\ a_9 \end{Bmatrix}, \qquad a_i = \begin{Bmatrix} u_i \\ v_i \\ w_i \\ \alpha_i \\ \beta_i \end{Bmatrix} \qquad (i = 1, 2, \ldots, 9). \tag{4}$$

N is the shape function matrix of the nine-node superparametric shell element $N = [\bar{N}_1 \cdots \bar{N}_k \cdots \bar{N}_9]$, where

$$\bar{N}_k = \begin{bmatrix} N_k & 0 & 0 & N_k\varsigma \frac{h_k}{2} \bar{V}_{1k}^x & -N_k\varsigma \frac{h_k}{2} \bar{V}_{2k}^x \\ 0 & N_k & 0 & N_k\varsigma \frac{h_k}{2} \bar{V}_{1k}^y & -N_k\varsigma \frac{h_k}{2} \bar{V}_{2k}^y \\ 0 & 0 & N_k & N_k\varsigma \frac{h_k}{2} \bar{V}_{1k}^z & -N_k\varsigma \frac{h_k}{2} \bar{V}_{2k}^z \end{bmatrix} \quad (k = 1, 9). \tag{5}$$

According to the perturbation theory, we assume that the cylindrical shell's vibration is small around the equilibrium position. The non-linear plate-shell theory [26] for large deflection is used to handle the cylindrical shell before it reaches the equilibrium state by centrifugal forces. The strain–displacement relation in local co-ordinate x, y, z is

$$\bar{\varepsilon} = \begin{Bmatrix} \varepsilon_x \\ \varepsilon_y \\ \gamma_{xy} \\ \gamma_{xz} \\ \gamma_{yz} \end{Bmatrix} = \begin{Bmatrix} \dfrac{\partial u}{\partial x} \\ \dfrac{\partial v}{\partial y} \\ \dfrac{\partial u}{\partial y} + \dfrac{\partial v}{\partial x} \\ \dfrac{\partial u}{\partial z} + \dfrac{\partial w}{\partial x} \\ \dfrac{\partial v}{\partial z} + \dfrac{\partial w}{\partial y} \end{Bmatrix} + \begin{Bmatrix} \dfrac{1}{2}\left[\left(\dfrac{\partial u}{\partial x}\right)^2 + \left(\dfrac{\partial v}{\partial x}\right)^2 + \left(\dfrac{\partial w}{\partial w}\right)^2\right] \\ \dfrac{1}{2}\left[\left(\dfrac{\partial u}{\partial y}\right)^2 + \left(\dfrac{\partial v}{\partial y}\right)^2 + \left(\dfrac{\partial w}{\partial y}\right)^2\right] \\ \dfrac{\partial u}{\partial x}\dfrac{\partial u}{\partial y} + \dfrac{\partial v}{\partial x}\dfrac{\partial v}{\partial y} + \dfrac{\partial w}{\partial x}\dfrac{\partial w}{\partial y} \\ \dfrac{\partial u}{\partial y}\dfrac{\partial u}{\partial z} + \dfrac{\partial v}{\partial y}\dfrac{\partial v}{\partial z} \\ \dfrac{\partial u}{\partial z}\dfrac{\partial u}{\partial x} + \dfrac{\partial v}{\partial z}\dfrac{\partial v}{\partial x} \end{Bmatrix} = \bar{\varepsilon}_l + \bar{\varepsilon}_n, \tag{6}$$

where the non-linear strain component is

$$\bar{\varepsilon}_n = \tfrac{1}{2} S R \tag{7}$$

and

$$S = \begin{bmatrix} H_1^{\mathrm{T}} & 0 & 0 \\ 0 & H_2^{\mathrm{T}} & 0 \\ H_2^{\mathrm{T}} & H_1^{\mathrm{T}} & 0 \\ 0 & H_3^{\mathrm{T}} & H_2^{\mathrm{T}} \\ H_3^{\mathrm{T}} & 0 & H_1^{\mathrm{T}} \end{bmatrix}, \tag{8}$$

$$R = \begin{bmatrix} H_1 \\ H_2 \\ H_3 \end{bmatrix} = T\bar{a}, \tag{9}$$

with

$$H_1 = \begin{bmatrix} \dfrac{\partial u}{\partial x} \\ \dfrac{\partial v}{\partial x} \\ \dfrac{\partial w}{\partial x} \end{bmatrix}, \quad H_2 = \begin{bmatrix} \dfrac{\partial u}{\partial y} \\ \dfrac{\partial v}{\partial y} \\ \dfrac{\partial w}{\partial y} \end{bmatrix}, \quad H_1 = \begin{bmatrix} \dfrac{\partial u}{\partial z} \\ \dfrac{\partial v}{\partial z} \\ \dfrac{\partial w}{\partial z} \end{bmatrix}, \tag{10}$$

$$T = [T_1 \quad T_2 \cdots T_4], \qquad T_i = \begin{bmatrix} \dfrac{\partial N_i}{\partial x} I \\ \dfrac{\partial N_i}{\partial y} I \\ \dfrac{\partial N_i}{\partial z} I \end{bmatrix}. \tag{11}$$

The differential representation of equation (7) is

$$\mathrm{d}\bar{\varepsilon}_n = \tfrac{1}{2}\,\mathrm{d}SR + \tfrac{1}{2}S\,\mathrm{d}R = ST\,\mathrm{d}\bar{a} = B_n\,\mathrm{d}\bar{a}. \tag{12}$$

The matrix of strain–displacement relationship is taken in the form

$$B = B_l + B_n. \tag{13}$$

The elements of the matrix B are not constant for non-linear shells with large deformation. From equations (12), (13) and (6), we obtain

$$B_n = ST. \tag{14}$$

The tangential stiffness matrix in geometric non-linear problem has the expression

$$K\,\mathrm{d}\bar{a} = [K_0 + K_\sigma]\,\mathrm{d}\bar{a} = \mathrm{d}P = \int_V B^{\mathrm{T}}\,\mathrm{d}\bar{\sigma}\,\mathrm{d}V + \int_V \mathrm{d}B^{\mathrm{T}}\,\bar{\sigma}\,\mathrm{d}V, \tag{15}$$

because

$$\bar{\sigma} = D\bar{\varepsilon} = DB\bar{a}. \tag{16}$$

We have

$$K_0 = \int_V B^{\mathrm{T}} DB\,\mathrm{d}V, \tag{17}$$

$$K_\sigma\,\mathrm{d}\bar{a} = \int_V \mathrm{d}B^{\mathrm{T}}\bar{\sigma}\,\mathrm{d}V = \int_V \mathrm{d}B_n^{\mathrm{T}}\,\bar{\sigma}\,\mathrm{d}V. \tag{18}$$

Substituting equation (14) into equation (18) gives

$$K_\sigma\,\mathrm{d}\bar{a} = \int_V T^{\mathrm{T}}\,\mathrm{d}S^{\mathrm{T}}\,\bar{\sigma}\,dV. \tag{19}$$

From equations (8) and (9), we have

$$\mathrm{d}S^{\mathrm{T}}\bar{\sigma} = [\sigma]\,T\,\mathrm{d}\bar{a}, \tag{20}$$

where

$$\sigma = \begin{bmatrix} \sigma_{xx}I & \tau_{xy}I & \tau_{xz}I \\ \tau_{yx}I & \sigma_{yy}I & \tau_{yz}I \\ \tau_{zx}I & \tau_{zy}I & \sigma_{zz}I \end{bmatrix}. \tag{21}$$

Substituting equation (20) into equation (19), we obtain

$$K_\sigma = \int_V T^{\mathrm{T}}[\sigma]\,T\,\mathrm{d}V. \tag{22}$$

We assume that the cylindrical shell's vibration is small around the new equilibrium position. The shell is assumed to be rotating at a constant angular velocity $\bar{\Omega}$ about its center axis which gets across a reference point O. A location vector can be defined as $\bar{r}_0$ from point Q of the shell to the fixed reference point O, the corresponding elasticity deformation vector is $\bar{\delta}(r_0, t)$, the velocity vector of deformation is $\dot{\bar{\delta}}$, the total displacement of the point Q is

$$\bar{r} = \bar{r}_0 + \bar{\delta} \tag{23}$$

and the corresponding velocity is

$$\bar{v} = \bar{\Omega} \times \bar{r} + \dot{\bar{\delta}}, \tag{24}$$

where

$$\bar{r}_0 = \begin{Bmatrix} r_{0x} \\ r_{0y} \\ r_{0z} \end{Bmatrix}, \quad \bar{\delta} = \begin{Bmatrix} u \\ v \\ w \end{Bmatrix}, \quad \bar{\Omega} = \begin{Bmatrix} \Omega_x \\ \Omega_y \\ \Omega_z \end{Bmatrix}, \tag{25}$$

Ω_x, Ω_y and Ω_z are the components $\bar{\Omega}$ in global co-ordinate x, y and x respectively.

The kinetic energy of this point is

$$\Delta T = \frac{1}{2}\Delta m(\bar{\Omega} \times \bar{r}) \times (\bar{\Omega} \times \bar{r}) + \Delta m(\bar{\Omega} \times \bar{r})\dot{\bar{\delta}} + \frac{1}{2}\Delta m \dot{\bar{\delta}}\dot{\bar{\delta}}. \tag{26}$$

For the whole element the kinetic energy can be written as follows:

$$T = \frac{1}{2}\int_V (\dot{\bar{\delta}}^{\mathrm{T}}\bar{\delta} + 2\dot{\bar{\delta}}^{\mathrm{T}}\underline{\Omega}\bar{\delta} + \bar{\delta}^{\mathrm{T}}\underline{\Omega}^{\mathrm{T}}\underline{\Omega}\bar{\delta} + 2\bar{r}_0^{\mathrm{T}}\underline{\Omega}^{\mathrm{T}}\dot{\bar{\delta}} + 2\bar{r}_0^{\mathrm{T}}\underline{\Omega}^{\mathrm{T}}\underline{\Omega}\bar{\delta})\,\mathrm{d}m, \tag{27}$$

where

$$\underline{\Omega} = \begin{bmatrix} 0 & -\Omega_z & \Omega_y \\ \Omega_z & 0 & -\Omega_x \\ -\Omega_y & \Omega_x & 0 \end{bmatrix}. \tag{28}$$

By substituting equation (3) into equation (27), we obtain

$$T = \frac{1}{2}\dot{\bar{a}}^{\mathrm{T}}M\dot{\bar{a}} + \frac{1}{2}\dot{\bar{a}}G\bar{a} + \frac{1}{2}\bar{a}^{\mathrm{T}}K_c\bar{a} + \bar{a}^{\mathrm{T}}I + \dot{\bar{a}}^{\mathrm{T}}A + \dot{\bar{a}}^{\mathrm{T}}J\bar{a}, \tag{29}$$

where

$$M = \int_V N^{\mathrm{T}}N\,\mathrm{d}m, \quad G = 2\int_V N^{\mathrm{T}}\underline{\Omega}N\,\mathrm{d}m, \quad K_c = \int_V N^{\mathrm{T}}\underline{\Omega}^{\mathrm{T}}\underline{\Omega}N\,\mathrm{d}m. \tag{30}$$

K_c is the matrix due to the rotation of particular element and G is the matrix due to Coriolis acceleration. The expressions of I, A and J will not be given in this paper because they do not appear in the motion equation.

The element potential energy is

$$V = \tfrac{1}{2}\,\bar{a}^{\mathrm{T}} K \bar{a}. \tag{31}$$

From equations (29) and (31), using Hamilton's principle, the perturbation motion equation of shells about their equilibrium position is obtained

$$M\ddot{\bar{a}} + G\dot{\bar{a}} + (K - K_c)\bar{a} = 0, \tag{32}$$

where $K = [K_0 + K_\sigma]$ can be obtained from equations (17) and (22).

3. RESULTS AND DISCUSSION

The shell discussed in this paper is a thick cylindrical shell rotating about its center axis. The boundary conditions are free at both ends (Figure 1). The cylindrical shell has the following geometric properties and material properties, which are the same as that used in reference [25]. The only difference is that this is a rotating cylindrical shell now: $l = 0{\cdot}254$ m, $r = 0{\cdot}09525$ m, $t = 0{\cdot}0381$ m, $E = 2{\cdot}07 \times 10^{11}$ N/m^2, $\nu = 0{\cdot}28$, $\rho = 7{\cdot}86 \times 10^3$ kg/m^3.

3.1. COMPARISON WITH WANG'S RESULTS [25] FOR A NON–ROTATING CYLINDRICAL SHELL

In order to verify the program, we have calculated the stationary cylinder to compare with the results of Wang [25]. The comparison results are presented in Table 1.

From Table 1, it is observed that a good agreement between the present calculated results and the results of literature [25] has been obtained.

3.2. THREE-DIMENSIONAL MODE SHAPES AND FREQUENCIES OF ROTATING CYLINDRICAL SHELL

The modes of stationary thick cylinders were classified into eight categories by Wang and Williams [25]. However, no work on the three-dimensional mode shapes of a thick rotating cylinder has been carried out.

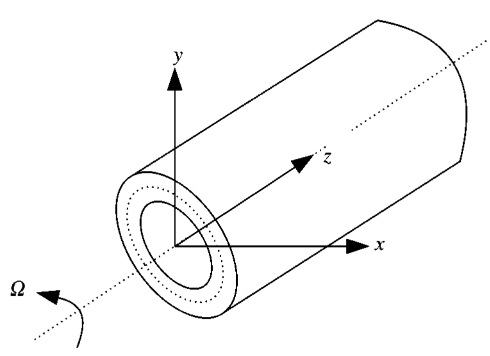

Figure 1. Geometry of a thick rotating cylindrical shell.

TABLE 1

The frequencies and vibrational modes of thick cylinder

Mode	Frequency (Hz)			Mode description		
	$f_{present}$	$f_{reference\,[25]}$	Error%†	n	m	Mode type
1	2573	2570	0·12	2	0	Pure radial
2	2950	2962	− 0·41	2	1	Radial shearing
3	6239	6286	− 0·75	1	1	Axial bending
4	6320	6291	− 0·97	0	1	Torsion
5	7134	7104	0·42	1	2	Global bending
6	8096	8149	− 0·65	0	0	Extensional
7	11 266	11 536	− 0·34	0	0	Longitudinal
8	12 653	12 616	0·29	1	1	Circumferential

† error $= 100 \times (f_{pre} - f_{reference\,(25)})/f_{reference\,[25]}$.

A simple equation for the rotating circular ring has been derived by Endo *et al.* [9] with an assumption of inextensional deformation. This equation is reproduced here as

$$\omega^* = \frac{\omega}{\omega_0} = \frac{2n}{n^2 + 1\omega_0}\frac{\Omega}{\omega_0} \mp \left(1 + \frac{n^2(n^2-1)^2}{(n^2+1)^2}\frac{\Omega}{\omega_0}\right)^{1/2}, \tag{33}$$

where ω is the frequency of the shell rotating at a speed Ω, ω_0 is the frequency of the shell when $\Omega = 0$, and n is the circumferential wave number, Equation (33) is quoted by many authors, and its results are in good agreement with the experimental results when the rotating speed is not too high. Another assumption applied in deriving equation (33) is that the vibrational displacement itself is much smaller than the thickness of the ring but the product terms of the initial tension due to rotation and vibrational strains should not be neglected. This assumption is valid for shells rotating at low speed.

Table 2 shows the results of shell rotating with speed $\Omega = 50$ Hz. The frequencies obtained by equation (33) are also shown in the table. It is observed that the percentage errors between the present results and the results from equation (33) are small.

In Table 2, n is half the number of circumferential nodes, and m is the number of longitudinal nodes. The u_r, u_i and u_z are average displacements that correspond to the radial, tangential and longitudinal directions of node, respectively. They are defined as follows:

$$u_j = 100 \times \sqrt{\frac{1}{k}\sum_{i=1}^{k} u_{ji}^2} \bigg/ \left(\sum_j \sqrt{\frac{1}{k}\sum_{i=1}^{k} u_{ji}^2}\right), \quad j = r, t, z, \tag{34}$$

where k is the whole number of finite element nodes of cylindrical shell. u_{ji} is the displacement of node i corresponding to the j direction. It can be seen from Table 2 that several combinations of the same n and m exist in the frequency range such as modes 11, 12, 14 and 15. It is clearly impossible for stationary shell. But for the cylindrical shell rotating about its center axis, two different frequencies named, respectively, the backward wave and the forward wave frequencies have the same n and m due to rotation. It is difficult to identify which is a pair among modes 11, 12, 14, 15. Using the method presented by Wang and Williams [25], we calculated the displacement ratio of each mode. Then modes 11, 12, 14, 15 can be classified into two pairs, mode 11 and 12, modes 14 and 15. In n and m columns of

TABLE 2

The frequencies and vibrational modes of thick cylinder rotating around the center axis with speed $\Omega = 50$ Hz

Mode	Frequency (Hz)			Mode description			Displacement ratio
	$f_{present}$	$f_{equation\ [25]}$	Error%†	n	m	Mode type	$u_r:u_t:u_{z(present)}$
1	2477	2488	− 0·44	2	0	Pure radial	52:26:0
2	2580	2568	0·47	2	0	Pure radial	50:25:0
3	2866	2872	− 0·21	2	1	Radial shearing	35:19:13
4	2958	2951	0·24	2	1	Radial shearing	34:18:12
5	6202	6177	0·40	1	1 (0)	Axial bending	24:12:27
6	6253	6277	− 0·38	1	1 (0)	Axial bending	24:12:26
7	6315	6316	0·00	0	1	Torsion	0:36:0
8	6991	6983	0·11	1	2	Global bending	12:6:4
9	7075	7083	− 0·11	1	2	Global bending	12:6:4
10	8759	8759	0·00	0	2	Extensional	13:0:1
11	9502	9473	0·31	2	3 (0)	Axial bending	12:6:19
12	9526	9553	− 0·28	2	3 (0)	Axial bending	12:6:19
13	11,216	11,216	0·00	0 (0)	2 (0)	Longitudinal	16:0:30
14	11,726	11,702	0·21	2	3	Radial shearing	9:2:4
15	11,759	11,782	0·20	2	3	Radial shearing	9:2:4
16	12,474	12,475	0·00	1	1	Circumferential	6:8:3
17	12,578	12,575	0·00	1	1	Circumferential	6:8:3

† error $= 100 \times (f_{present} - f_{equation\ (33)})/f_{equation\ (33)}$.

Table 2, the number in the parenthesis is the description method of three-dimensional mode quoted from the literature [25], where it has different meanings for different modes.

Figure 2 shows eight categories for the mode of a rotating cylindrical shell. It is concluded that the method presented by Wang and Williams [25] is suitable to identify the three-dimensional modes of rotating thick cylindrical shells. In addition, several points can be obtained:

1. u_z of pure radial mode approaches zero.
2. u_r and u_z of torsion mode approach zero.
3. u_t of extensional and longitudinal modes approaches zero.
4. u_z of axial bending and longitudinal modes is the greatest among $u_r\, u_t\, u_z$.
5. u_r of pure radial and radial shearing modes is the greatest among $u_r\, u_t\, u_z$.
6. u_t of torsion and circumferential modes is the greatest among $u_r\, u_t\, u_z$.

3.3. THE EFFECT OF ROTATIONAL SPEED ON FREQUENCY CHARACTERISTICS OF THE ROTATING CYLINDRICAL SHELL FOR DIFFERENT MODES

In this section, studies focus on the variations of frequency at various three-dimensional modes of free vibration and rotating speed of the F-F thick cylindrical shell. The present results are shown in Figures 3–9. The ordinate and the abscissa, respectively, show the normalized natural frequency, $\omega^*(=\omega/\omega_0)$ and normalized rotating speed, $\Omega^*(=\Omega/\omega_0)$. The effects of rotation on frequencies for pure radial and radial shearing modes are shown in Figures 3–5. The effects of rotation on frequencies for circumferential, global bending and

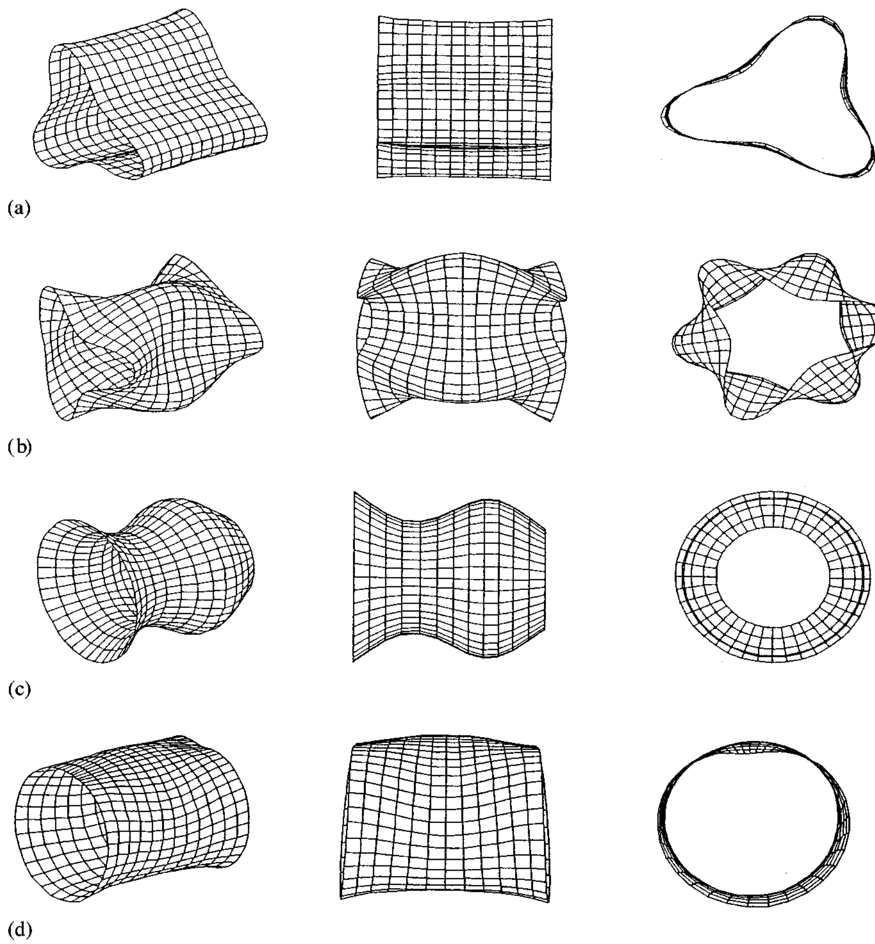

Figure 2. Eight categories for the mode of a rotating cylindrical shell with rotating speed $\Omega = 50$ Hz. (a) pure radial mode $m = 0, n = 3$; (b) radial shearing mode $m = 2, n = 3$; (c) extensional mode $m = 3, n = 0$; (d) circumferential mode $m = 1, n = 1$; (e) axial bending mode $m = 0, n = 2$; (f) global bending mode $m = 3, n = 1$; (g) torsion mode $m = 1, n = 0$; (h) longitudinal mode $m = 0, n = 0$.

axial bending modes are shown in Figures 6, 7 and 8, respectively. The effects of rotation of frequencies for extensional, longitudinal and torsion modes are shown in Figure 9. Curves of five kinds of modes (pure radial, radial shearing, circumferential, global bending and axial bending modes) are presented in Figures 10 and 11 in order to compare on with the others.

Figure 3 illustrates the influence of the rotating speed on frequency characteristics of a rotating shell for pure radial ($m = 0, n = 2$) and radial shearing modes ($m = 1, n = 2$) and ($m = 2, n = 2$). We can see from equation (33) that the result of ω^* is not affected by the number of longitudinal nodes m. This is because Equation (33) was derived on the assumption of a rotating ring. From Figure 3, it can be seen that there is very little difference between the natural frequencies of three modes at low rotational speed. However, this difference increases when the rotational speed increases. The curves of frequency for pure radial mode ($m = 0, n = 2$) lie out of other modes' curves, curves of radial shearing mode ($m = 1, n = 2$) lie between the pure radial ($m = 0, n = 2$) and the radial shearing ($m = 2, n = 2$) modes and curves of radial shearing mode ($m = 2, n = 2$) lie innermost.

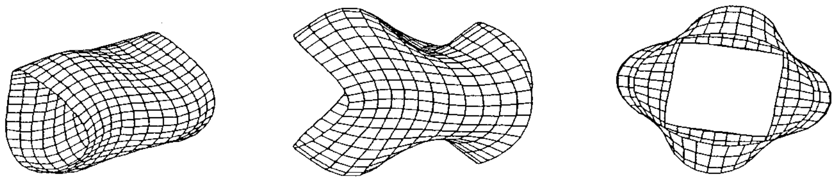

(e)

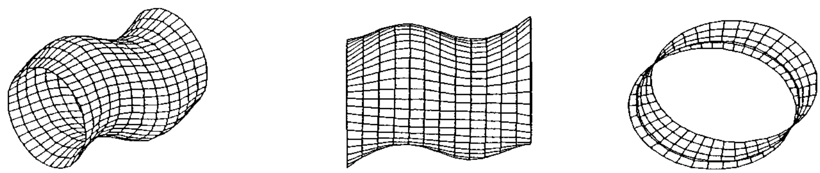

(f)

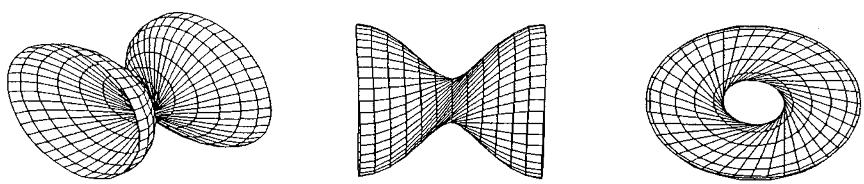

(g)

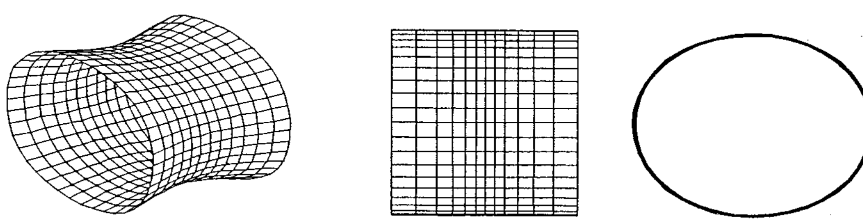

(h)

Figure 2. Continued

Figure 4 illustrates the influence of the rotating speed on frequency characteristics of a rotating shell for pure radial ($m = 0, n = 3$) and radial shearing modes ($m = 1, n = 3$) and ($m = 2, n = 3$). Figure 5 illustrates the results for pure radial ($m = 0, n = 4$) and radial shearing ($m = 1, n = 4$) modes. The conclusion of Figure 3 can also be derived from Figures 4 and 5. From Figures 3–5, the trend of curves in good agreement with the result obtained earlier in references [9, 22, 23] its shows, and it is observed that the deviation of curves of different modes with large circumferential wave number n is less than that with small circumferential wave number n. So it is concluded that the normalized frequency of the rotating thick cylindrical shell for pure radial and radial shearing modes with large circumferential wave number n can be expressed as the normalized rotational speed. Another conclusion from Figures 3–5 is that the curves corresponding to larger m lie out of the curves of smaller m for the same n.

Figure 6 shows the relation between the natural frequency and the rotational speed for circumferential mode ($m = 1, n = 1$) and ($m = 0, n = 1$). The curve for this kind of mode has not been investigated before, because it is difficult to identify the circumferential mode by the usual method. The natural frequencies associated with the backward waves are found to increase monotonically with the rotational speed, and for forward waves, the natural

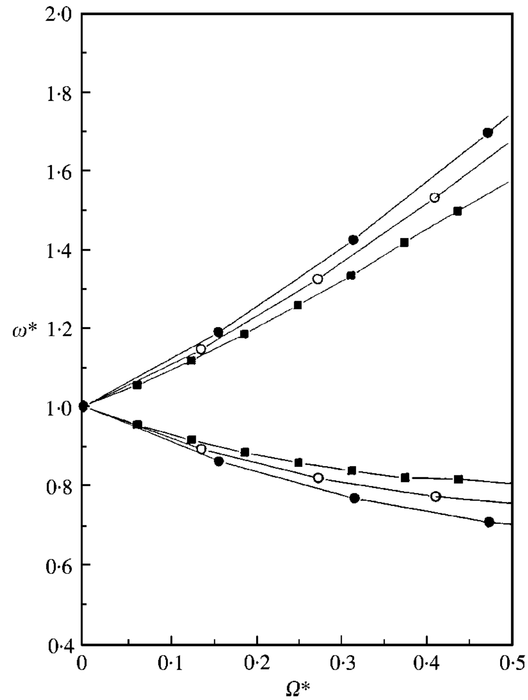

Figure 3. Natural frequency ω^*(Hz) as a function of the rotating angular velocity Ω^*(Hz) at different modes ($m = 0, n = 2$) for pure radial mode; $m = 1, n = 2$ and $m = 2, n = 2$ for radial shearing mode) for an F-F rotating thick cylindrical shell: —●—, $m = 0, n = 2$, pure radial mode; —○—, $m = 1, n = 2$, radial shearing mode; —■—, $m = 2, n = 2$, radial shearing mode.

frequencies decrease gradually with the rotational speed. The curves of frequency for mode ($m = 0, n = 1$) lie out of that of mode ($m = 1, n = 1$).

Figure 7 shows the results of global bending mode ($m = 2, n = 1$) and ($m = 3, n = 1$). It is observed that the curves of the backward and forward waves are basically linear when Ω^* is not too high. The same result can be obtained from equation (33). But when $\Omega^* > 0{\cdot}3$, the curves of backward wave are non-linear, and it is observed that m has no influence on the normalized natural frequency from equation (33), while there is an obvious effect of m on the forward and backward waves along with the increase or rotating speed in the present result. This is because the inextensional assumption adopted by equation (33) is not suitable for a thick cylinder. From Figure 7, it can be found that the curves of frequency for mode ($m = 2, n = 1$) lie out of that for mode ($m = 3, n = 1$).

The results of axial bending mode ($m = 0, n = 1$), ($m = 0, n = 2$) and ($m = 1, n = 0$) are shown in Figure 8. The mode description method of Reference [25] is used here. When using the past mode description method, they are ($m = 1, n = 1$), ($m = 3, n = 2$) and ($m = 2, n = 1$) respectively. Due to the difficulty in identifying the mode, the effects of rotation on frequency for this kind of mode have not been investigated so far. The natural frequencies associated with the backward wave are all found to increase monotonically with the rotational speed, and the values of the natural frequency for ($m = 0, n = 1$) and ($m = 0, n = 2$) increase more quickly than that for ($m = 1, n = 1$). For forward waves, the natural frequencies of ($m = 1, n = 1$) decrease with the rotational speed, and those of ($m = 0, n = 1$) and ($m = 0, n = 2$) decrease first and then almost remain unchanged. It is concluded that the influences of both m and n on forward and backward waves are obvious.

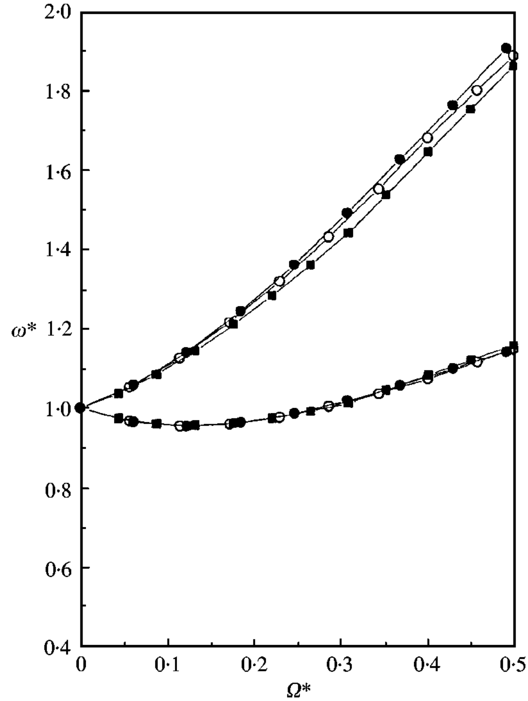

Figure 4. Natural frequency ω^*(Hz) as a function of the rotating angular velocity Ω^*(Hz) at different modes ($m = 0, n = 3$) for pure radial mode; $m = 1, n = 2$ and $m = 2, n = 3$ for radial shearing mode) for an F-F rotating thick cylindrical shell: —●—, $m = 0, n = 3$, pure radial mode; —○—, $m = 1, n = 3$, radial shearing mode; —■—, $m = 2, n = 3$, radial shearing mode.

Two points of intersection can be found in Figure 8, which are the only ones occurring for all the computed results. It is easy to understand the upper point because it is the curve of ($m = 3, n = 2$) intersecting that of ($m = 2, n = 1$) (from the old mode description method). But further study is needed to explain the intersection point of curve ($m = 1, n = 1$) and curve ($m = 2, n = 1$) (from that old mode description method).

Figure 9 shows the variation of the natural frequency with the rotational speed for extensional ($m = 3, n = 0$), longitudinal ($m = 0, n = 0$) and torsion modes ($m = 1, n = 0$). It is observed that only one curve for each mode existed when $n = 0$. From equation (33) one can see that when $n = 0$ there is no change for the frequency parameter ω^* with Ω^*. But the present results show that: for extensional mode ($m = 3, n = 0$), there is a slight difference in the frequency when the rotating speed increases; for longitudinal mode ($m = 0, n = 0$), the natural frequencies increase gradually with the rotating speed; for torsion mode ($m = 1, n = 0$), the natural frequencies decrease with the rotating speed. From equation (17), (22) and (32), one can see that the stiffness matrix K of the rotating cylindrical shell includes three components: K_0, the stiffness matrix due to geometric shape and material properties of the cylindrical shell: K_σ, the stiffness matrix due to pre-stress when rotating, which increases the total stiffness; K_c, the stiffness matrix due to variation of centrifugal force, which reduces the stiffness. One cannot decide whether the frequencies of one mode are higher or lower with rotating speed unless calculation is done.

Curves of five kinds of modes (pure radial, radial shearing, circumferential, global bending and axial bending modes) are shown in Figure 10 for backward wave and Figure 11 for forward wave. From Figures 10 and 11, one can see that the frequency differences are

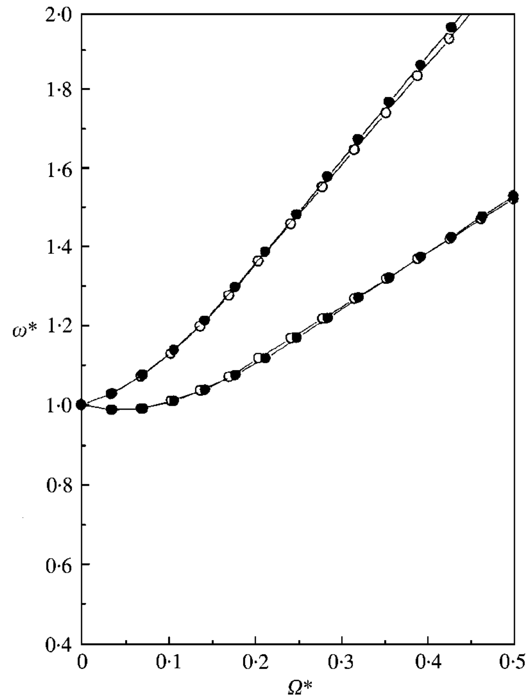

Figure 5. Natural frequency ω^*(Hz) as a function of the rotating angular velocity Ω^*(Hz) at different modes ($m = 0, n = 4$) for pure radial mode; $m = 1, n = 4$ for radial shearing mode) for an F-F rotating thick cylindrical shell: —●—, $m = 0, n = 4$, pure radial mode; —○—, $m = 1, n = 4$, radial shearing mode.

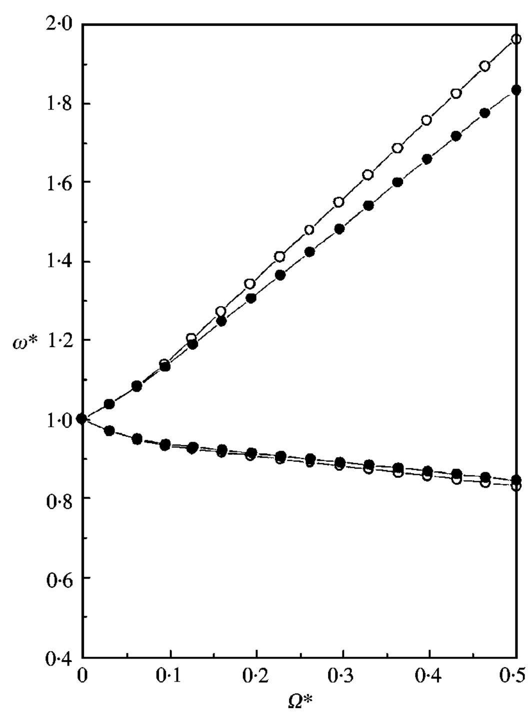

Figure 6. Natural frequency ω^*(Hz) as a function of the rotating angular velocity Ω^*(Hz) at different modes ($m = 1, n = 1$ and $m = 0, n = 1$ for circumferential mode) for an F-F rotating thick cylindrical shell: —●—, $m = 1, n = 1$, circumferencial mode; —○—, $m = 0, n = 1$, circumferential mode.

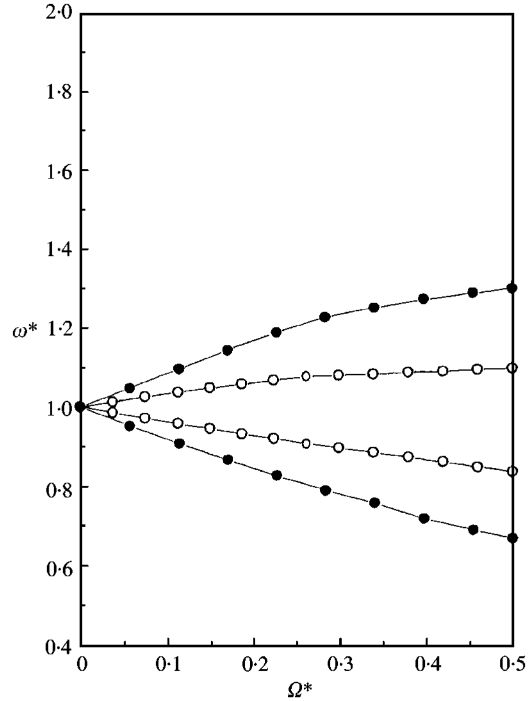

Figure 7. Natural frequency ω^*(Hz) as a function of the rotating angular velocity Ω^*(Hz) at different modes ($m = 2, n = 1$ and $m = 3, n = 1$ for global bending mode) for an F-F rotating thick cylindrical shell: —●—, $m = 2, n = 1$, global bending mode; —○—, $m = 3, n = 1$, global bending mode.

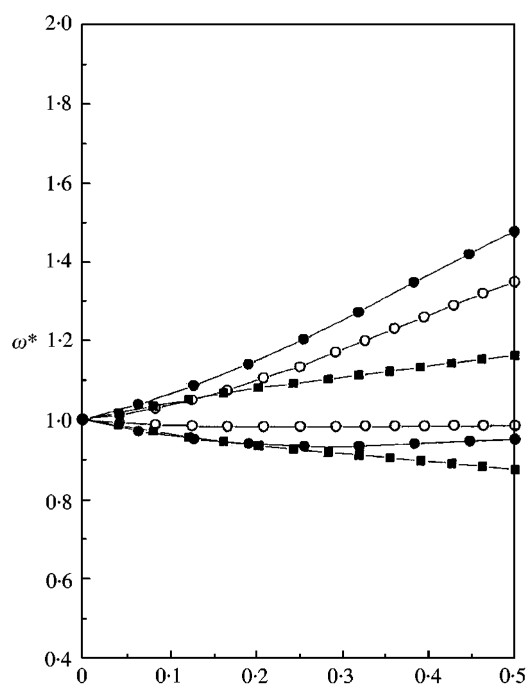

Figure 8. Natural frequency ω^*(Hz) as a function of the rotating angular velocity Ω^*(Hz) at different modes ($m = 0, n = 1$ and $m = 0, n = 2$ and $m = 1, n = 1$ for axial bending mode) for an F-F rotating thick cylindrical shell: —●—, $m = 0, n = 1$, axial bending mode; —○—, $m = 0, n = 2$, axial bending mode; —■—, $m = 1, n = 1$, axial bending mode.

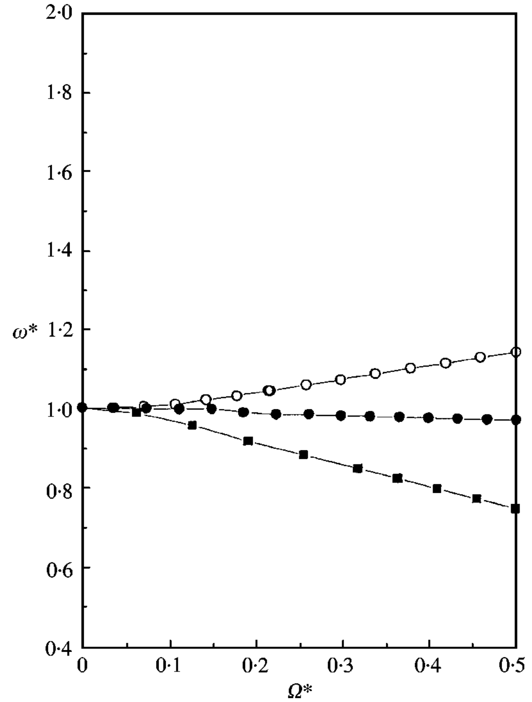

Figure 9. Nature frequency ω^*(Hz) as a function of the rotating angular velocity Ω^*(Hz) at different modes ($m = 3$, $n = 0$ for extensional mode; $m = 0$, $n = 0$ for longitudinal mode; $m = 1$, $n = 0$ for torsion mode) for an F-F rotating thick cylindrical shell: —●—, $m = 3$, $n = 0$, extensional mode; —○—, $m = 0$, $n = 0$, longitudinal mode; —■— $m = 1$, $n = 0$, torsion mode.

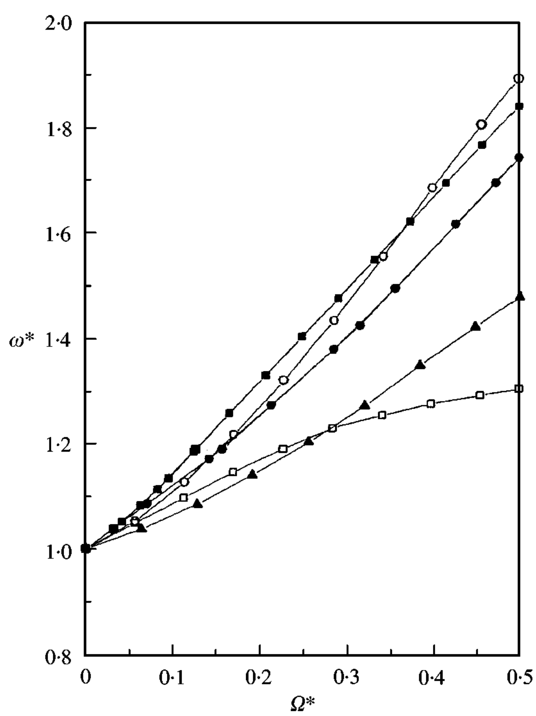

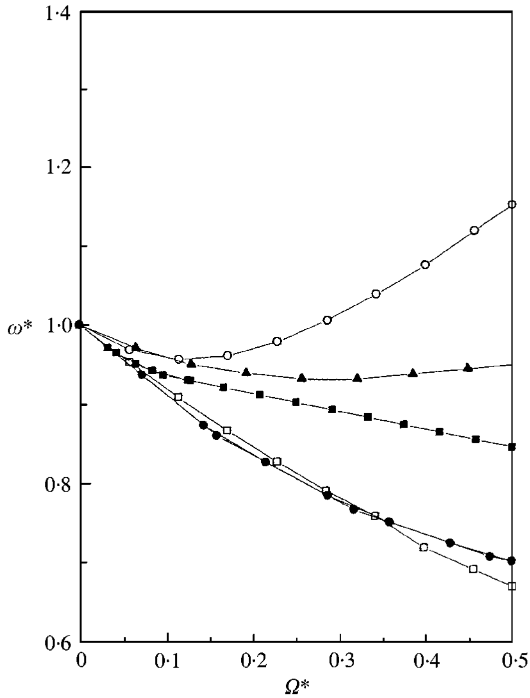

Figure 11. Nature frequency ω^*(Hz) as a function of the rotating angular velocity Ω^*(Hz) at five kinds of modes for forward wave: —●—, $m = 0, n = 2$, pure radial mode; —○—, $m = 1, n = 3$, radial shearing mode; —■—, $m = 0, n = 1$, circumferencial mode; —□—, $m = 2, n = 1$, global bending mode; —▲—, $m = 0, n = 1$, axial bending mode.

small for different modes when the rotating velocity is small, but these differences increase with the increase of the rotating velocity. So the frequency differences especially at high rotating speed are often the focus of many investigators.

4. CONCLUSIONS

Rotating thick cylindrical shells have been analyzed by using the nine-node superparametric finite element method. The finite element form of rotating cylindrical shells has been deduced. The shear and axial deformation and rotatory inertia have been considered in the finite element model. The effects of Coriolis acceleration, centrifugal force, initial tension and geometric non-linearity due to large deformation have been included in the physical model. The non-linear plate-shell theory for large deflection is used to handle the cylindrical shell before it reaches the equilibrium state by centrifugal force, and then a linear approximation is employed.

For a thick cylindrical shell with F-F boundary condition the effect of rotation on different three-dimensional modes is investigated. Eight categories of the mode for

◀

Figure 10. Nature frequency ω^*(Hz) as a function of the rotating angular velocity Ω^*(Hz) at five kinds of modes for backward wave: —●—, $m = 0, n = 2$, pure radial mode; —○—, $m = 1, n = 3$, radial shearing mode; —■—, $m = 0, n = 1$, circumferencial mode; —□—, $m = 2, n = 1$, global bending mode; —▲—, $m = 0, n = 1$, axial bending mode.

a rotating thick cylindrical shell are presented in this paper. Based on the analysis, the following conclusions can be drawn:

1. There are eight categories of modes for a rotating thick cylindrical shell. They can be identified by using half of the circumferential node number n, longitudinal node number m and the displacement distribution.
2. For pure radial and radial shearing modes, the normalized frequency of the rotating thick cylindrical shell with large circumferential wave number n can be expressed as the normalized rotational speed, and the curves corresponding to larger m lie out of the curves of smaller m for the same n.
3. For global bending mode, the curves of the backward and forward waves are basically linear at low speed, but they are non-linear when the rotating speed is high. There is an obvious effect of m on the curves of forward and backward waves along with the increase of rotating speed.
4. For axial bending mode, the influences of both m and n on forward and backward wave curves are obvious.
5. There are three kinds of modes when $n = 0$. They are the extensional, the longitudinal and the torsion modes. Only one value of the natural frequency for each mode exists at one rotating speed when $n = 0$. It cannot be decided whether the frequencies of one mode increase or decrease with the rotating speed when $n = 0$ unless calculation is done.
6. The frequency differences are small for different modes when the rotating velocity is small, but these differences increase with the increase of the rotating velocity.

ACKNOWLEDGMENT

This research is financially supported by a project from the National Key Basic Research Special Fund (No. G1998020316) and National Natural Science Foundation of China (Grant Number 19990510).

REFERENCES

1. G. H. BRYAN 1890 *Proceedings of the Cambridge Philosophical Society* **7**, 101–111. On the beats in the vibration of revolving cylinder or bell.
2. D. TARANTO and M. LESSON 1964 *Journal of Applied Mechanics* **31**, 700–719. Coriolis acceleration effect on vibration of a rotating thin-walled circular cylinder.
3. A. V. SRINIVASAN and G. F. LAUTERBACH 1971 *Journal of Engineering for Industry* **93**, 1229–1232. Travelling waves in rotating cylindrical shells.
4. A. ZOHAR and J. ABOUDI 1973 *International Journal of Mechanical Science* **15**, 269–278. The free vibrations of thin circular finite rotating cylinder.
5. J. PADOVAN 1973 *Journal of Sound Vibration* **31**, 469–482. Natural frequencies of rotating prestressed cylinders.
6. J. PADOVAN 1975 *International Journal of Solid Structures* **11**, 1367–1380. Travelling waves vibrations and buckling of rotating anisotropic shells of revolution by finite elements.
7. J. PADOVAN 1975 *Computer Structures* **5**, 145–154. Numerical analysis of asymmetric frequency and buckling eigenvalues of pre-stressed rotating anisotropic shells of revolution.
8. T. SAITO and M. ENDO 1986 *Journal of Sound and Vibration* **107**, 17–28. Vibration of finite length rotating cylindrical shells.
9. M. ENDO, K. HATAMURA, M. SAKATA and O. TANIGUCH 1984 *Journal of Sound and Vibration* **92**, 261–272. Flexural vibration of a thin rotating ring.
10. O. RAND and Y. STAVSKY 1991 *International Journal of Solid Structures* **28**, 831–843. Free vibrations of spinning composite cylindrical shells.

11. K. Y. LAM and C. T. LOY 1995 *Journal of Sound Vibration* **186**, 23–25. Analysis of rotating laminated cylindrical shells by different thin shell theories.
12. K. Y. LAM and C. T. LOY 1994 *Composite Engineering* **4**, 1153–1167. On vibrations of thin rotating laminated composite cylindrical shells.
13. K. Y. LAM and C. T. LOY 1995 *International Journal of Solids and Structures* **32**, 647–663. Free vibrations of a rotating multi-layered cylindrical shell.
14. K. Y. LAM and C. T. LI 1999 *Composites Part B* **30**, 135–144. On free vibration of a rotating truncated circular orthotropic conical shell.
15. K. Y. LAM and C. T. LI 1997 *International Journal of Solids and Structures* **34**, 2183–2196. Vibration analysis of a rotating truncated circular conical shell.
16. K. Y. LAM and C. T. LI 1999 *Journal of Sound and Vibration* **223**, 171–195. Influence of boundary conditions on the frequency characteristics of a rotating truncated circular conical shell.
17. K. Y. LAM and C. T. LI 2000 *International Journal of Mechanical Sciences* **44**, 213–236. Influence of initial pressure on frequency characteristics of a rotating truncated circular shell.
18. H. LI and K. Y. LAM 1998 *International Journal of Mechanical Science* **40**, 443–459. Frequency characteristics of a thin rotating cylindrical shell using the generalized differential quadrature method.
19. S. C. HUANG and B. S. HSU 1990 *Journal of Sound and Vibration* **136**, 215–228. Resonant phenomena of a rotating cylindrical shell subjected to a harmonic moving load.
20. T. Y. NG and K. Y. LAM 1998 *Journal of Sound and Vibration* **214**, 513–529. Parametric resonance of a rotating cylindrical shell subjected to periodic axial loads.
21. Y. CHEN, H. B. ZHAO and Z. P. SHEN 1993 *Journal of Sound and Vibration* **160**, 137–160. Vibrations of high speed rotating shells with calculations for cylindrical shells.
22. K. R. SIVADAS and N. GANESAN 1994 *Journal of Vibration Acoustics* **116**, 198–202. Effect of rotation on vibration of moderately thick circular cylindrical shells.
23. K. R. SIVADAS 1995 *Journal of Sound and Vibration* **186**, 99–109. Vibration analysis of pre-stressed rotating thick circular conical shell.
24. R. K. SINGAL and K. WILLIAMS 1998 *ASME Journal of Vibration, Acoustics, Stress and Reliability in Design* **110**, 533–537. A theoretical and experimental study of vibrations of thick circular cylindrical shell and rings.
25. H. WANG and K. WILLIAMS 1998 *Journal of Vibration and Acoustics* **120**, 371–376. A Vibrational mode analysis of free finite–length thick cylinders using the finite element method.
26. E. HINTON and D. OWEN 1984 *Finite Element Software for Plates and Shells*. UK: Swansea. Prineridge Pr.